Anisotropy effect on multi-Gaussian beam propagation in turbulent ocean

Yalçın Ata[1,*] and Yahya Baykal[2]

[1]*TÜBİTAK Defense Industries Research and Development Institute (TÜBİTAK SAGE), P.K. 16 Mamak, 06261 Ankara, Turkey*

[2]*Çankaya University, Department of Electrical-Electronics Engineering, Yukarıyurtçu mah. Mimar Sinan cad., 06790 Ankara, Turkey*

**Corresponding author: ylcnata@gmail.com*

Received April 5, 2018; accepted June 13, 2018; posted online July 27, 2018

Average transmittance of multi-Gaussian (flat-topped and annular) optical beams in an anisotropic turbulent ocean is examined analytically based on the extended Huygens–Fresnel principle. Transmittance variations depending on the link length, anisotropy factor, salinity and temperature contribution factor, source size, beam flatness order of flat-topped beam, Kolmogorov microscale length, rate of dissipation of turbulent kinetic energy, rate of dissipation of the mean squared temperature, and thickness of annular beam are examined. Results show that all these parameters have effects in various forms on the average transmittance in an anisotropic turbulent ocean. Hence, the performance of optical wireless communication systems can be improved by taking into account the variation of average transmittance versus the above parameters.

OCIS codes: 010.4455, 010.7060, 010.4450, 350.5500, 010.1330.

doi: 10.3788/COL201816.080102.

The performance of the optical wireless systems is strictly dependent on the propagation medium constituents, which attenuate and degrade the wave. Turbulence is a significant phenomenon that affects an optical beam, which is also affected by absorption and scattering effects. There are numerous studies analyzing optical wave propagation in atmospheric turbulence in various aspects, such as the intensity[1], scintillation[2], transmittance[3–8], and beam spreading[9]. Temperature and wind variations are dominant factors in atmospheric refractive index characteristics, and these variations are defined by Kolmogorov and non-Kolmogorov spectra. In the ocean, salinity and temperature become the main factors that develop turbulence. Nikishov and Nikishov defined the contribution of salinity and temperature fluctuations to the refractive index spectrum in the ocean[10]. After this work, many studies examining optical turbulence characteristics in the ocean have appeared in the literature. Optical turbulence characteristics in the ocean are investigated for various entities, as the scintillation, structure function, intensity, polarization, and field correlation[11–16]. Anisotropic turbulent medium is also another noteworthy subject for research. There are several studies investigating anisotropy characteristics of the turbulent spectrum in different media[17–20]. These studies[17–20] cover the log-amplitude correlation function for spherical wave propagation through anisotropic non-Kolmogorov atmosphere, average polarization of the electromagnetic Gaussian Schell model beams propagating through anisotropic non-Kolmogorov turbulence, polarization of quantization Gaussian Schell beams through anisotropic non-Kolmogorov turbulence of the marine atmosphere, and effects of anisotropic turbulence on the average polarizability of Gaussian Schell model quantized beams through an ocean link. In our earlier studies, we have reported in anisotropic oceanic turbulence, the intensity fluctuations of spherical optical beams[21], the intensity fluctuations[22], and the bit error rate (BER) of asymmetrical Gaussian beams[23]. In these works, the observation is that anisotropy in the turbulent ocean causes reductions in the intensity fluctuations and BER. As the result, optical wireless communications systems operating in anisotropic oceanic turbulence will have better performance than the ones operating in isotropic oceanic turbulence. Results show that anisotropy affects optical wave propagation significantly. For the optical wave propagating in the z direction, since the anisotropic oceanic turbulence exhibits asymmetrical spatial frequencies usually in the x, y directions, its effects on the physical entities of propagation, such as the average intensity, intensity fluctuations, and beam spreading, are quite different when compared to the effects imposed by isotropic oceanic turbulence. Thus, it is important to scrutinize the anisotropic turbulence structures and their effects on optical wave propagation in the ocean.

In this study, we have examined the average transmittance of multi-Gaussian beams, which include the flat-topped and annular, in anisotropic turbulent ocean against the oceanic turbulence parameters, including the anisotropy factor and the multi-Gaussian beam source parameters. We believe that this study will contribute to the optical wireless system performance analysis in oceanic optical telecommunication links.

The average transmittance of a turbulent medium depending on the intensity profiles is defined as

$$\langle \tau(L)\rangle = \frac{\langle I(L)\rangle}{I^v(L)}, \tag{1}$$

where L is the link length, $\langle \tau(L)\rangle$ denotes the ensemble average over the medium statistics, $\langle I(L)\rangle$ is the on-axis average intensity profile in the oceanic turbulent medium, and $I^v(L)$ is the on-axis intensity in vacuum. According to the extended Huygens–Fresnel principle, the on-axis average intensity profile of an optical beam at the receiver plain is obtained to be[1]

$$\begin{aligned}\langle I(L)\rangle = \left(\frac{1}{\lambda L}\right)^2 \int_{-\infty}^{\infty}\int_{-\infty}^{\infty} \mathrm{d}^2\boldsymbol{s}_1 \mathrm{d}^2\boldsymbol{s}_2\, u(\boldsymbol{s}_1)u^*(\boldsymbol{s}_2) \\ \times \exp\left[\frac{jk}{2L}(|\boldsymbol{s}_1|^2 + |\boldsymbol{s}_2|^2)\right] \\ \times \langle \exp[\psi(\boldsymbol{s}_1) + \psi^*(\boldsymbol{s}_2)]\rangle,\end{aligned} \tag{2}$$

where λ is the wavelength, $k = 2\pi/\lambda$ is the wavenumber, $\boldsymbol{s} = (s_x, s_y)$ is the transverse coordinate at the source plane, $u(\boldsymbol{s})$ is the incident field of the optical beam, $\psi(\boldsymbol{s})$ is the complex random phase term of oceanic turbulence, $j = \sqrt{-1}$, and $*$ represents the complex conjugate. The incident field of a multi-Gaussian beam is defined as[8,24]

$$u(\boldsymbol{s}, z = 0) = \sum_{n=1}^{N} A_n \exp(-k\alpha_n|\boldsymbol{s}|^2), \tag{3}$$

where N is the beam flatness order, A_n and α_n are the complex amplitude and source size of the nth Gaussian beam, $\alpha_n = \frac{1}{2k\alpha_{sn}^2} + \frac{j}{2F_n}$, and F_n is the focal length. In this study, collimated flat-topped and annular beams are taken into account, thus, $F_n = \infty$ is taken, and $\alpha_n = \frac{1}{2k\alpha_{sn}^2} + \frac{j}{2F_n}$ transforms to $\alpha_n = \frac{1}{2k\alpha_{sn}^2}$. By using the expressions in Ref. [24], the parameters for the flat-topped Gaussian beam are obtained as $A_n = \frac{(-1)^{n-1}}{N}\binom{N}{n}$, where $\binom{N}{n} = \frac{N!}{n!(N-n)!}$, and the parameters of the collimated annular beam are found from $u(\boldsymbol{s}, z = 0) = A\exp\left(-\frac{1}{2\alpha_{s1}^2}|\boldsymbol{s}|^2\right) - A\exp\left(-\frac{1}{2\alpha_{s2}^2}|\boldsymbol{s}|^2\right)$, where $N = 2$, $A_1 = -A_2 = A$, $\alpha_1 = \frac{1}{2k\alpha_{s1}^2}$, and $\alpha_2 = \frac{1}{2k\alpha_{s2}^2}$; α_{s1} and α_{s2} are the source sizes of the outer and inner Gaussian beams.

The ensemble average of the complex random phase term in anisotropic turbulent oceanic medium is

$$\langle \exp[\psi(\boldsymbol{s}_1) + \psi^*(\boldsymbol{s}_2)]\rangle = \exp\left(-\frac{|\boldsymbol{s}_1 - \boldsymbol{s}_2|^2}{\rho_{oc\xi}^2}\right), \tag{4}$$

where $\rho_{oc\xi}$ is the coherence length of the anisotropic turbulent ocean, which is found to be[20]

$$\rho_{oc\xi} = \left[\frac{\pi^2}{3}k^2 L\xi^{-4}\int_0^{\infty} \kappa_\xi^3 \varphi_n(\kappa_\xi)\mathrm{d}\kappa_\xi\right]^{-1/2}. \tag{5}$$

Here, ξ is the anisotropy factor, $\kappa_\xi = \sqrt{\kappa_z^2 + \xi^2\kappa_p^2}$ is the magnitude of the spatial frequency, and $\kappa_p^2 = \kappa_x^2 + \kappa_y^2$, where κ_x, κ_y, and κ_z are spatial frequency components in the x, y, and z directions, respectively. According to the Markov approximation, we assume that the κ_z component in the anisotropic oceanic turbulent medium can be ignored due to delta correlation and spatial frequency, and $\kappa_\xi = \xi\kappa_p$[22]. The power spectrum of the anisotropic turbulent ocean is[10]

$$\begin{aligned}\varphi_n(\kappa_\xi, \xi) = \frac{0.388\times 10^{-8}\varepsilon^{-1/3}\xi^2 X_T}{w^2}\kappa_\xi^{-11/3}[1 + 2.35(\kappa_\xi\eta)^{2/3}] \\ \times (w^2 e^{-A_T\delta} + e^{-A_S\delta} - 2we^{-A_{\mathrm{TS}}\delta}),\end{aligned} \tag{6}$$

where ε is the rate of dissipation of turbulent kinetic energy, varying from 1×10^{-1} m^2/s^3 in the most active regions, surf zones, straits, and where there are very rapid tidal currents, to 1×10^{-10} m^2/s^3 in the abyssal ocean[25]; X_T is the dissipation of the mean squared temperature varying from 10^{-2} K^2/s in surface water to 1×10^{-10} K^2/s in deep water, η is the Kolmogorov microscale length given as $\eta = (v^3/\varepsilon)^{1/3}$[26], v is the kinematic viscosity, w is the parameter, which gives the temperature and the salinity contribution factor to turbulence, $w = 0$ when the salinity driven turbulence is dominant, and $w = -5$ when the temperature driven turbulence is dominant, $A_T = 1.863\times 10^{-2}$, $A_S = 1.9\times 10^{-4}$, $A_{\mathrm{TS}} = 9.41\times 10^{-3}$, $\delta = 8.284(\kappa_\xi\eta)^{-4/3} + 12.978(\kappa_\xi\eta)^2$. Substituting Eq. (6) into Eq. (5), after some calculations, the spatial coherence length of the anisotropic turbulent ocean medium can be expressed as[20]

$$\begin{aligned}\rho_{oc\xi} = \xi|w|1.802\times 10^{-7}k^2 L(\varepsilon\eta)^{-1/3} \\ \times X_T[(0.483w^2 - 0.835w + 3.380)]^{-1/2}.\end{aligned} \tag{7}$$

Note that the term $|w|$ in Eq. (7) appears as $|w|^{-1}$ in Ref. [20], which is a typographical error.

Inserting the multi-Gaussian beam incident field expression given by Eq. (3) into Eq. (2), the average intensity of the multi-Gaussian beam is found to be

$$\begin{aligned}\langle I(L)\rangle = \left(\frac{k}{2\pi L}\right)^2 \sum_{l_1=1}^{N}\sum_{l_2=1}^{N}\int_{-\infty}^{\infty}\mathrm{d}s_{1x}\int_{-\infty}^{\infty}\mathrm{d}s_{1y}\int_{-\infty}^{\infty}\mathrm{d}s_{2x}\int_{-\infty}^{\infty}\mathrm{d}s_{2y} \\ \times A_{l_1}A_{l_2}\exp\left[\left(-k\alpha_{l_1} - \frac{1}{\rho_{oc\xi}^2} + \frac{jk}{2L}\right)s_{1x}^2 + \frac{2}{\rho_{oc\xi}^2}s_{1x}s_{2x}\right] \\ \times \exp\left[\left(-k\alpha_{l_1} - \frac{1}{\rho_{oc\xi}^2} + \frac{jk}{2L}\right)s_{1y}^2 + \frac{2}{\rho_{oc\xi}^2}s_{1y}s_{2y}\right] \\ \times \exp\left[\left(-k\alpha_{l_2} - \frac{1}{\rho_{oc\xi}^2} - \frac{jk}{2L}\right)s_{2x}^2\right] \\ \times \exp\left[\left(-k\alpha_{l_2} - \frac{1}{\rho_{oc\xi}^2} - \frac{jk}{2L}\right)s_{2y}^2\right].\end{aligned} \tag{8}$$

The integrals in Eq. (8) are evaluated using the integral formula given in Eq. 3.323.2 of Ref. [27], which is

$$\int_{-\infty}^{\infty} \exp(-p^2x^2 \pm qx)\mathrm{d}x = \exp\left(\frac{q^2}{4p^2}\right)\frac{\sqrt{\pi}}{p}, \qquad \mathrm{Re}\,(p^2) > 0, \tag{9}$$

and the average intensity of the multi-Gaussian beam is found as

$$\langle I(L)\rangle = \left(\frac{k}{2\pi L}\right)^2 \sum_{l_1=1}^{N} \times \sum_{l_2=1}^{N} \frac{A_{l_1}A_{l_2}\pi^2}{\left(k\alpha_{l_1} + \frac{1}{\rho_{oc\xi}^2} - \frac{jk}{2L}\right)\left(k\alpha_{l_2} + \frac{1}{\rho_{oc\xi}^2} + \frac{jk}{2L}\right) - \frac{1}{\rho_{oc\xi}^4}}. \tag{10}$$

Using the coherence length in vacuum, $\rho_0 = \infty$, the intensity in vacuum will be

$$I^v(L) = \left(\frac{k}{2\pi L}\right)^2 \sum_{l_1=1}^{N}\sum_{l_2=1}^{N} \frac{A_{l_1}A_{l_2}\pi^2}{\left(k\alpha_{l_1} - \frac{jk}{2L}\right)\left(k\alpha_{l_2} + \frac{jk}{2L}\right)}. \tag{11}$$

Finally, substituting Eqs. (10) and (11) into Eq. (1), the average transmittance of the anisotropic turbulent ocean is obtained.

The variations of the average transmittance in the anisotropic turbulent ocean are given for various parameters. Results are obtained analytically. Beams in all of the figures are taken symmetrically, so the source sizes in the x and y directions are chosen equally as $\alpha_{sx} = \alpha_{sy} = \alpha_s$. Figures 1–8 reflect the flat-topped beam transmittance characteristics in the anisotropic turbulent ocean, whereas Fig. 9 gives the annular beam transmittance properties. In all of the presented figures, the propagation wavelength is chosen as $\lambda = 0.417$ μm, which is suitable for underwater applications, since it is a window wavelength.

In Fig. 1, the transmittance variation is plotted against the anisotropic factor for different w values. It is found that the transmittance increases as the anisotropic characteristic of the turbulence increases in the ocean. It is seen that the salinity driven turbulence affects transmittance severely in comparison to the temperature driven turbulence. When salinity is almost completely dominant, i.e., $w = -0.1$, the transmittance approaches its minimum level. Besides complete salinity dominant turbulence, when turbulence is isotropic ($\xi = 1$), the transmittance is at the zero level.

Figure 2 reflects the transmittance variance against the anisotropy factor for various beam source sizes. In Fig. 2, when the curves are compared at the same anisotropy factor value, it is seen that the flat-topped beam having a larger source size exhibits higher transmittance than the flat-topped beam having a smaller source size; i.e., in Fig. 2, the flat-topped beam having $\alpha_s = 6$ cm has the largest transmittance value. Transmittance change for the small beam source sizes (for example, from $\alpha_s = 1$ cm to $\alpha_s = 2$ cm) is significantly high, whereas the

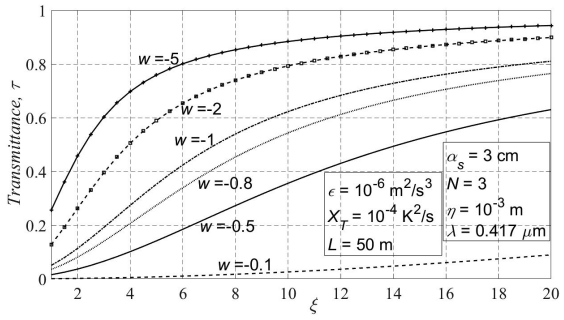

Fig. 1. Average transmittance of the flat-topped beam versus anisotropy factor for various salinity and temperature contribution factors.

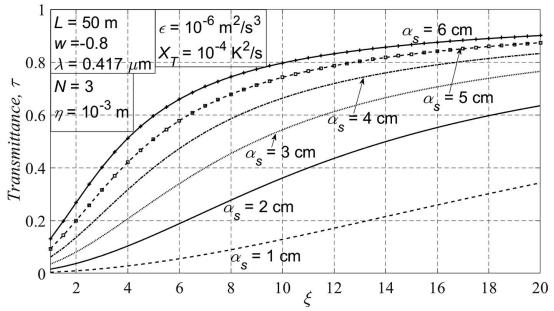

Fig. 2. Average transmittance of the flat-topped beam versus anisotropy factor for various beam source sizes.

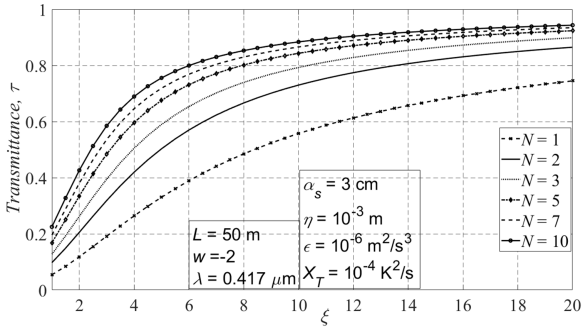

Fig. 3. Average transmittance of the flat-topped beam versus anisotropy factor for various beam flatness orders.

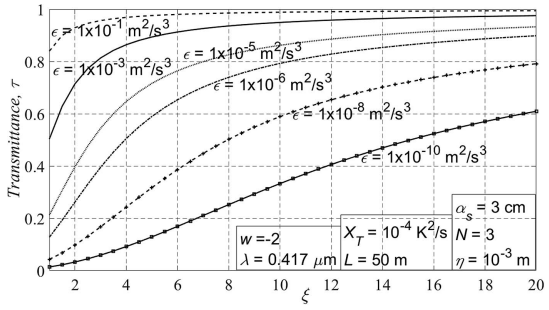

Fig. 4. Average transmittance of the flat-topped beam versus anisotropy factor for various rates of dissipation of turbulent kinetic energy.

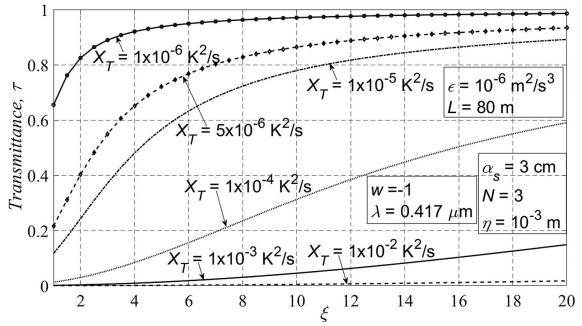

Fig. 5. Average transmittance of the flat-topped beam versus anisotropy factor for various rates of dissipation of the mean squared temperature.

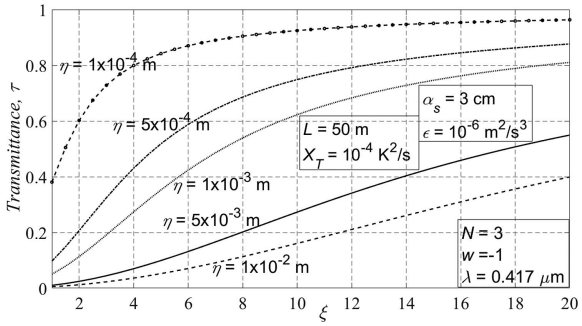

Fig. 6. Average transmittance of the flat-topped beam versus anisotropy factor for various Kolmogorov microscale lengths.

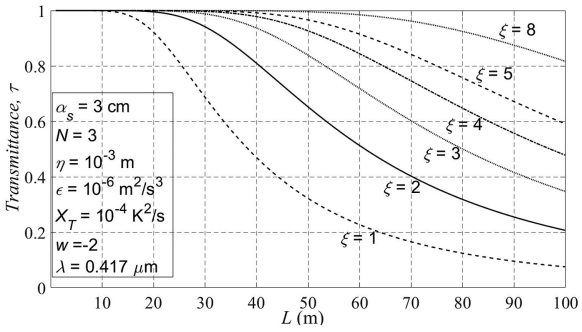

Fig. 7. Average transmittance of the flat-topped beam versus the link length for various anisotropy factors.

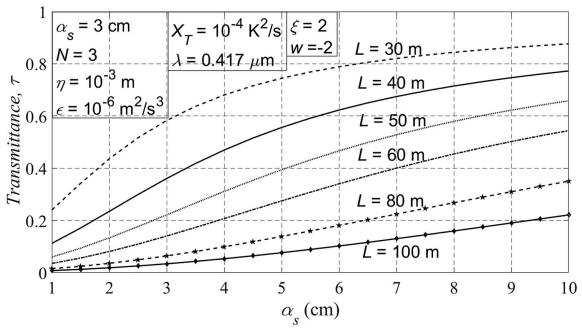

Fig. 8. Average transmittance of the flat-topped beam versus source size for various link lengths.

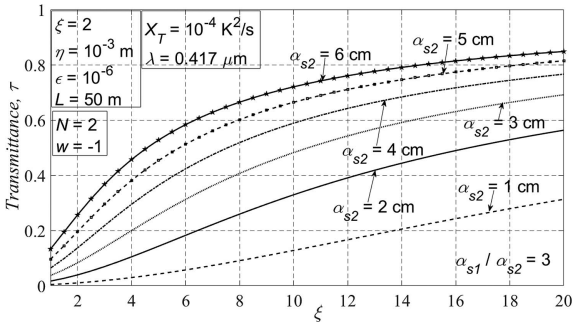

Fig. 9. Average transmittance of the annular beam versus anisotropy factor for various source sizes when the inner and outer source size ratios are fixed.

transmittance changes less for large beam sizes (from $\alpha_s = 5$ cm to $\alpha_s = 6$ cm). This shows that the propagation with the larger beam sizes is more power efficient underwater. This is physically reasonable, since a larger beam spread occurs when the flat-topped beam of the smaller size propagates in anisotropic oceanic turbulence, which means that for smaller size flat-topped beams, smaller transmittance values are obtained, as compared to the transmittance values obtained for larger size flat-topped beams.

Figure 3 denotes that the increase in the order of beam flatness changes the transmittance of the underwater optical communication system in a positive manner, similar to the case of the increase in anisotropy. It is seen from Fig. 3 that when $N > 5$ and $\xi > 10$, the changes in the transmittance are smaller, while the changes are larger for smaller values of both flatness order and anisotropy. It is seen that the transmittance differs slightly after a certain level of beam flatness and anisotropy factor. In Fig. 3, the physics behind the trend, which shows that in a given anisotropic oceanic turbulent medium flatter beams have larger transmittances, is based on the fact that beams with flatter field profiles diffract less, thus contributing more to transmittance.

We note that the multi-Gaussian beams are formed by the weighted summation of two or more Gaussian beams, such as the flat-topped beam, or by the difference of two Gaussian beams, such as the annular beam. Even though the multi-Gaussian beams are composed of single Gaussian beams, their intensity profiles are completely different than the intensity profile of a single Gaussian beam. For example, the annular beam has a ring type intensity structure, and, if formed by many Gaussian beams, flat-topped beams have truncated flat intensity patterns. As the result, in any medium, the transmittances obtained for multi-Gaussian beams are quite different than the transmittance obtained for a single Gaussian beam. This fact is clearly seen in Fig. 3, in which, at the same anisotropy factor, the transmittances of flat-topped beams formed by two or more Gaussian beams, i.e., the curves for $N > 2$, are favorable when compared to the transmittance of a single Gaussian beam, i.e., the curve for $N = 1$.

This finding indicates that in terms of obtaining a high transmittance level in a given anisotropic oceanic turbulence medium, the use of a flat-topped beam will be much more advantageous than the use of a single Gaussian beam.

It is concluded from Fig. 4 that, being valid for all the anisotropic factor values ξ, as the rate of dissipation of the turbulent kinetic energy ε increases, the transmittance starts to increase. When ε takes its maximum value as $\varepsilon = 10^{-1}$ $\mathrm{m}^2/\mathrm{s}^3$ and when the oceanic turbulence is isotropic ($\xi = 1$), the transmittance approximately reaches 0.84 at the receiver, which is 50 m from the source. At the same ε value, there is almost no loss, while the anisotropy factor takes larger values.

Figure 5 provides the variations of transmittance versus the anisotropy factor for various rates of dissipation of mean squared temperature values. It is concluded that the transmittance has its lowest level when the rate of dissipation of mean squared temperature takes its maximum value, i.e., when the beam propagation is close to the surface. The transmittance values jump to higher values in the transition from isotropic to anisotropic turbulence at the smaller values of the rate of dissipation of mean squared temperature.

It is inferred from Fig. 6 that as the Kolmogorov microscale length increases transmittance decreases. At the large value of the anisotropy factor, the rate of increase in transmittance is higher for small values of the Kolmogorov microscale length and is smaller when the Kolmogorov microscale length is larger. As also given above, the Kolmogorov microscale length is expressed by the equality $\eta = (v^3/\varepsilon)^{0.25}$, v being the kinematic viscosity. Thus, the trends in Fig. 6 should be evaluated by considering this equality, i.e., in Fig. 6, since ε is fixed, change in η also refers to change in the kinematic viscosity of the anisotropic oceanic turbulence.

In Fig. 7, the transmittance versus the link length is given for various anisotropy factor values. It is seen from Fig. 7 that the underwater optical communication system link length without any attenuation is approximately 10 m when the turbulence characteristic is isotropic. This lossless transmission distance is pulled up with every increase in the anisotropy factor level. When the oceanic turbulence is isotropic, the transmittance starts to decrease sharply upon an increase in the distance. When oceanic turbulence is more anisotropic, the same levels of transmittance occur at longer distances.

The variation of the transmittance versus the beam source size for different link lengths is given in Fig. 8. It is seen that thicker beams yield higher transmittance in comparison to the thinner beams. As the propagation distance increases, an increase in the beam source size will increase the performance of the underwater optical communication system. Figure 8 also shows that the transmittance at several tens of meters in the underwater environment may still be at an acceptable level in terms of power loss due to turbulence effects.

Finally, transmittance variations versus anisotropy factors for various annular beam source sizes are shown in Fig. 9 when the ratio of the outer size and the inner size of the beam is fixed and is taken as $\alpha_{s1}/\alpha_{s2} = 3$. It can be inferred from Fig. 9 that the beam with the higher inner source sizes yields higher transmittance, and the transmittance starts to increase as the thickness of the annular beam increases. The physical meaning of the results shown in Figs. 8 and 9 are similar to the physical reasoning provided above in the explanation for Fig. 2, i.e., larger size flat-topped beams at any link length (Fig. 8) and larger size annular beams at any anisotropy factor (Fig. 9) will experience smaller beam spread, resulting in larger transmittance values.

A common observation from Figs. 1–6, 8, and 9 is that under any oceanic turbulence and optical source beam parameters, as the ocean becomes more anisotropic, transmittance increases. This is physically explained by the fact that anisotropic oceanic turbulence possesses an asymmetrical eddy structure, having less dense continuum formation, leading to weaker turbulence when compared to the corresponding isotropic oceanic turbulence strength that has a symmetrical eddy structure. This means that for the same oceanic turbulence and source parameters in an anisotropic ocean, transmittance is degraded less than in an isotropic ocean, so the transmittance values are higher at larger anisotropy factors. The physical interpretations of the results in Figs. 1, 4, 5, and 7, respectively, are that, being valid for any anisotropic factor, at smaller w, smaller X_T, smaller L, or at larger ε, oceanic turbulence strength becomes weaker, yielding larger transmittance values.

In this Letter, the average transmittance of a multi-Gaussian beam in an anisotropic turbulent ocean is investigated. Results show that transmittance increases as the anisotropy factor, the beam flatness order, the beam source size, and the rate of dissipation of turbulent kinetic energy increase. The transmittance level decreases when the propagation distance, rate of dissipation of the mean squared temperature, and microscale length increase. Salinity dominates the transmittance adversely in an anisotropic ocean more than the temperature.

An important conclusion in this Letter is that the transmittance for both the flat-topped and annular beams increases as the anisotropy in the oceanic turbulence increases. Thus, the power performance of optical wireless applications is positively affected when the turbulent ocean has a higher anisotropy factor.

References

1. X. Chu, C. Qiao, and X. Feng, Opt. Laser Technol. **43**, 1150 (2011).
2. Y. Baykal, H. T. Eyyuboğlu, and Y. Cai, Appl. Opt. **48**, 1943 (2009).
3. Y. Ata and Y. Baykal, IEEE J. Sel. Area Commun. **33**, 1996 (2015).
4. Y. Ata and Y. Baykal, J. Mod. Opt. **58**, 1644 (2011).
5. Y. Ata, Waves Random Complex **24**, 431 (2014).
6. Y. Ata, Y. Baykal, and H. Gerçekcioğlu, Opt. Commun. **305**, 126 (2013).
7. Y. Baykal, Opt. Commun. **231**, 129 (2004).
8. H. T. Eyyuboğlu and Y. Baykal, Opt. Commun. **278**, 17 (2007).
9. G. Wu, H. Guo, S. Yu, and B. Luo, Opt. Lett. **35**, 715 (2010).

10. V. V. Nikishov and V. I. Nikishov, Int. J. Fluid Mech. Res. **27**, 82 (2000).
11. O. Korotkova, N. Farwell, and E. Shchepakina, Waves Random Complex Med. **22**, 260 (2012).
12. Y. Ata and Y. Baykal, J. Opt. Soc. Am. A **31**, 1552 (2014).
13. Y. Ata and Y. Baykal, Waves Random Complex **24**, 164 (2014).
14. O. Korotkova and N. Farwell, Opt. Commun. **284**, 1740 (2011).
15. W. Lu, L. Liu, and J. Sun, J. Opt. A **8**, 1052 (2006).
16. Y. Baykal, Opt. Commun. **393**, 29 (2017).
17. V. S. R. Gudimetla, R. B. Holmes, and J. F. Riker, J. Opt. Soc. Am. A **31**, 148 (2014).
18. Y. Zhao, Y. Zhang, and Q. Wang, Radioengineering **25**, 652 (2016).
19. Y. Zhao, Y. Zhang, Z. Hu, Y. Li, and D. Wang, Opt. Commun. **371**, 178 (2016).
20. Y. Li, Y. Zhang, Y. Zhu, and M. Chen, Appl. Opt. **55**, 5234 (2016).
21. Y. Baykal, J. Mod. Opt. **65**, 825 (2018).
22. Y. Baykal, Appl. Opt. **55**, 7462 (2016).
23. Y. Ata and Y. Baykal, Appl. Opt. **57**, 2258 (2018).
24. Y. Li, Opt. Lett. **27**, 1007 (2002).
25. S. A. Thorpe, *The Turbulent Ocean* (Cambridge University Press, 2005), p. 25.
26. F. Hanson and M. Lasher, Appl. Opt. **49**, 3224 (2010).
27. I. S. Gradshteyn and I. M. Ryzhik, *Tables of Integrals, Series and Products* (Academic, 2000).